

1 **Interactive network configuration maintains bacterioplankton**  
2 **community structure under elevated CO<sub>2</sub> in a eutrophic coastal**  
3 **mesocosm experiment**

4

5 Xin Lin<sup>†\*1</sup>, Ruiping Huang<sup>†1</sup>, Yan Li<sup>1</sup>, Futian Li<sup>1</sup>, Yaping Wu<sup>1,2</sup>, David A. Hutchins<sup>3</sup>,  
6 Minhan Dai<sup>1</sup>, Kunshan Gao<sup>\*1</sup>

7

8 **Institutions:**

9 <sup>1</sup> State Key Laboratory of Marine Environmental Science, College of Ocean & Earth Sciences, Xiamen  
10 University, Xiamen 361102, PR China.

11 <sup>2</sup>College of Oceanography, Hohai University, No.1 Xikang road, Nanjing 210000, China.

12 <sup>3</sup>Department of Biological Sciences, University of Southern California, 3616 Trousdale Parkway, AHF  
13 301, Los Angeles, CA 90089-0371, USA.

14

15 <sup>†</sup> These authors contributed equally to this work.

16 *Correspondence to:* Xin Lin (xinlinulm@xmu.edu.cn, TEL: +865922880171);

17 Kunshan Gao (ksgao@xmu.edu.cn, TEL: +865922187963)

18

19

20

21

22

23

24

25

26

27

28

29

30

31

32

1 **Abstract**

2       There is increasing concern about the effects of ocean acidification on marine biogeochemical and  
3 ecological processes and the organisms that drive them, including marine bacteria. Here, we examine the  
4 effects of elevated CO<sub>2</sub> on the bacterioplankton community during a mesocosm experiment using an  
5 artificial phytoplankton community in subtropical, eutrophic coastal waters of Xiamen, Southern China.  
6 Through sequencing the bacterial 16S rRNA gene V3-V4 region, we found that the bacterioplankton  
7 community in this subtropical, high nutrient coastal environment was relatively resilient to changes in  
8 seawater carbonate chemistry. Based on comparative ecological network analysis, we found that  
9 elevated CO<sub>2</sub> hardly altered the network structure of high abundance bacterioplankton taxa, but appeared  
10 to reassemble the community network of low abundance taxa. This led to relatively high resilience of the  
11 whole bacterioplankton community to the elevated CO<sub>2</sub> level and associated chemical changes. We also  
12 observed that the Flavobacteria group, which plays an important role in the microbial carbon pump,  
13 showed higher relative abundance under the elevated CO<sub>2</sub> condition during the early stage of the  
14 phytoplankton bloom in the mesocosms. Our results provide new insights into how elevated CO<sub>2</sub> may  
15 influence bacterioplankton community structure.

16

17

18 **Key words:** elevated CO<sub>2</sub>; mesocosm; bacterioplankton community; ecological network; Flavobacteria

19

## 1 **1 Introduction**

2 It is well established that ocean acidification is being caused by increased uptake of  
3 anthropogenically-derived carbon dioxide in the surface ocean. Consequently, it is predicted that under a  
4 “business-as-usual” CO<sub>2</sub> emission scenario, the present average surface pH value will drop 0.4 units over  
5 the next century (Gattuso et al., 2015). Despite a growing interest in the importance of the roles of marine  
6 bacterioplankton in ocean ecosystems and biogeochemical cycles, our current understanding of their  
7 responses to ocean acidification is still limited. Over half of autotrophically-fixed oceanic CO<sub>2</sub> is  
8 processed by heterotrophic bacteria and archaea through the microbial loop and carbon pump (Azam,  
9 1998; Jiao et al., 2010). Furthermore, marine bacterioplankton play an essential role in marine  
10 ecosystems and global biogeochemical cycles central to the biological chemistry of Earth (Falkowski et  
11 al., 2008). The null hypothesis is that elevated CO<sub>2</sub> will not affect biogeochemical processes (Liu et al.,  
12 2010; Joint et al., 2011), however more investigation is required. Ocean acidification mesocosm  
13 experiments provide good opportunities to explore the responses of marine bacteria to elevated CO<sub>2</sub>.  
14 Mesocosm studies conducted in the Arctic Ocean, Norway, Sweden and the coastal Mediterranean Sea  
15 using natural phytoplankton communities have often found that elevated CO<sub>2</sub> has little direct effect on  
16 the bacterioplankton community (Zhang et al., 2013; Ray et al., 2012, Roy et al., 2013; Baltar et al.,  
17 2015). In contrast, phytoplankton blooms induced by high CO<sub>2</sub> can sometimes have significant indirect  
18 effects on heterotrophic microbes, thus altering bacterioplankton community structure (Allgaier et al.,  
19 2008; Hutchins and Fu, 2017).

20 Although most mesocosm studies have showed that elevated CO<sub>2</sub> had an insignificant impact on  
21 bacterioplankton community structure, microcosm experiments have demonstrated that small changes in  
22 pH can have direct effects on marine bacterial community composition (Krause et al., 2012). Ocean

1 acidification experiments using natural biofilms showed bacterial community shifts, with decreasing  
2 relative abundance of Alphaproteobacteria and increasing relative abundance of Flavobacteriales (Witt et  
3 al., 2011). Coastal microbial biofilms grown at high CO<sub>2</sub> level also showed different community  
4 structures compared to those grown at ambient CO<sub>2</sub> level in a natural carbon dioxide vent ecosystem  
5 (Lidbury et al., 2012). Ocean acidification also affects the community structure of bacteria associated  
6 with corals. It has been reported that the relative abundance of bacteria associated with diseased and  
7 stressed corals increased under decreasing pH conditions (Meron et al., 2011). A very limited number of  
8 studies focused on the effects of ocean acidification on isolated bacterial strains have also been  
9 reported. Under lab conditions, growth of *Vibrio alginolyticus*, a species belonging to the class  
10 Gammaproteobacteria, was suppressed at low CO<sub>2</sub> levels (Labare et al., 2010). In contrast, stimulation of  
11 growth was observed for one Flavobacteria species under high CO<sub>2</sub> levels (Teira et al., 2012).

12 Taken together, results from mesocosm, microcosm and cultured isolate experiments indicate a  
13 potentially complex interaction between different groups of marine bacteria in response to elevated CO<sub>2</sub>.  
14 One promising method to elucidate these types of complex interactions is network analysis. Ecological  
15 network approaches have been successfully applied to investigate the complexity of interactions among  
16 zooplankton and phytoplankton from different trophic levels during the Tara Oceans Expedition project  
17 (Lima-mendez et al., 2015; Guidi et al., 2015). Elucidating the complex interactions between  
18 bacterioplankton and other marine organisms under anthropogenic perturbations will increase our  
19 understanding of their impact in a holistic way. Previous studies using ecological network analysis  
20 showed that elevated CO<sub>2</sub> significantly impacted soil bacterial/archaeal community networks, by  
21 decreasing the connections for dominant fungal species and reassembling unrelated fungal species in a  
22 grassland ecosystem (Tu et al., 2015). It was also reported using ecological network analysis that

1 elevated  $p\text{CO}_2$  did not significantly affect microbial community structure and succession in the Arctic  
2 Ocean, suggesting bacterioplankton community resilience to elevated  $p\text{CO}_2$  (Wang et al., 2016).

3 It has been reported that eutrophication problems in coastal regions lead to complex cross-linkages  
4 between ocean acidification and eutrophication (Cai et al., 2011). The occurrence of ocean acidification  
5 combined with other environmental stressors such as eutrophication can potentially produce synergistic  
6 or antagonistic effects on bacterioplankton that differ from those caused by ocean acidification alone.  
7 Although there are some reports from mesocosm experiments describing the response of bacteria to  
8 elevated  $\text{CO}_2$ , there are limited studies on how the bacterial community responds to ocean acidification in  
9 eutrophic marine environments. In this study, Illumina sequencing of the V3-V4 region of the bacterial  
10 16S rRNA gene was used to explore the effects of ocean acidification on bacterioplankton community  
11 composition and ecological network structure in a eutrophic coastal mesocosm experiment.

## 12 **2 Methods**

### 13 **2.1 Mesocosm setup and carbonate system manipulation**

14 The mesocosm experiment was conducted in the FOANIC-XMU (Facility for the Study of Ocean  
15 Acidification Impacts of Xiamen University) mesocosm platform located in Wuyuan Bay, Xiamen,  
16 Fujian province, East China Sea (N24°31'48", E118°10'47") during the months of December 2014 and  
17 January 2015 (Fig. S1). Each transparent thermoplastic polyurethane (TPU) cylindrical mesocosm bag  
18 was 3 m deep and 1.5 m wide (~4000 L total volume). After setting up the mesocosm bags within steel  
19 frames, in situ seawater from Wuyuan Bay was filtered through a 0.01 $\mu\text{m}$  water purifying system and  
20 used to simultaneously fill eight bags within 24 hours. The initial in situ seawater  $p\text{CO}_2$  in Wuyuan Bay  
21 was ~650  $\mu\text{atm}$ , due to the active decomposition of land-sourced organic compounds. In order to reach  
22 the target low  $p\text{CO}_2$  associated with ambient air (400 ppm),  $\text{Na}_2\text{CO}_3$  was added to each mesocosm to

1 increase dissolved inorganic carbon (DIC) and total alkalinity (TA) by 100  $\mu\text{mol/L}$  and 200  $\mu\text{mol/L}$   
2 respectively, based on carbonate system calculations (Lewis and Wallace, 1998). To adjust seawater to  
3 projected end of this century seawater conditions of  $\sim 1000$  ppm  $\text{CO}_2$ , about 5 L of  $\text{CO}_2$  saturated filtered  
4 seawater was added to 4 mesocosms (#2, #4, #7, #9), collectively considered to be the HC treatment,  
5 while the other 4 mesocosms (#1, #3, #6, #8) were considered to be the LC treatment. Throughout the  
6 experiment, HC mesocosms and LC mesocosms were bubbled with air containing 1000 ppm and 400  
7 ppm  $\text{CO}_2$ , respectively supplied by  $\text{CO}_2$  Enrichlors (CE-100B, Wuhan Ruihua Instrument & Equipment  
8 Ltd, China) at a flow rate of 4.8 L per minute. Two diatoms, *Phaeodactylum tricornutum* CCMA 106  
9 from the Centre for Collections of Marine Bacteria and Phytoplankton of the State Key Laboratory of  
10 Marine Environmental Science (Xiamen University, China), and *Thalassiosira weissflogii* CCMP 102  
11 from the Provasoli-Guillard National Center for Culture of Marine Phytoplankton (CCMP, USA), as well  
12 as the coccolithophorid *Emiliana huxleyi* CS-369 from the Commonwealth Scientific and Industrial  
13 Research Organization (CSIRO, Australia) were used as inoculum to construct a model phytoplankton  
14 community. The effects of ocean acidification on these phytoplankton species mentioned above have  
15 been intensively studied in the lab at physiological, biochemical and molecular levels. However, it is  
16 difficult to extrapolate the response of these species to ocean acidification in natural complex  
17 environments based on laboratory single species experiments (Busch et al., 2015). Our experiment was  
18 designed as an intermediary step between laboratory and natural community field experiments, with  
19 isolates of non-axenic phytoplankton being added to filtered natural waters. In this way, we were able to  
20 investigate the effect of OA on phytoplankton and bacterioplankton in naturally eutrophic waters while  
21 minimizing the complexity of shifting compositions of natural phytoplankton communities. Correlated  
22 data about the effects of ocean acidification on the artificial phytoplankton community using the same

1 mesocosm system are available in (Jin et al., 2015) and (Liu et al., 2017).

2 The initial concentration of both *P. tricornutum* and *T. weissflogii* was 10 cells/mL, and *E. huxleyi* was  
3 added at 20 cells/mL. The phytoplankton cultures were not axenic. The bacteria community  
4 composition in the inoculated phytoplankton culture is shown in Fig. S2. Bacteria were not detectable  
5 by flow cytometry in the filtered seawater just before inoculation. The three species of non-axenic  
6 phytoplankton with bacterioplankton were mixed and then inoculated into each mesocosm bag. Thus, we  
7 considered the initial bacterioplankton community to be the same or similar in each mesocosm bag  
8 because the phytoplankton culture with bacterioplankton were evenly distributed into each mesocosm  
9 bag for inoculation. The mesocosm and the CO<sub>2</sub> bubbling system were not sterile and not completely  
10 closed during the experiment. Therefore, natural bacterioplankton were undoubtedly introduced into the  
11 mesocosm system through aeration and air-sea exchange, and the bacterioplankton community in this  
12 mesocosm experiment was derived from both the bacteria added with the inoculated phytoplankton  
13 culture, and the natural local prokaryotic assemblage.

14 The use of the natural phytoplankton and bacterioplankton communities in this mesocosm experiment  
15 would better represent the effects of ocean acidification on natural phytoplankton and bacterioplankton  
16 communities. However, considering the highly eutrophic in situ seawater in Wuyuan Bay, it was  
17 impractical to use the in situ seawater with the in situ natural community (bacterioplankton,  
18 phytoplankton, zooplankton) directly without filtration, because of the dense phytoplankton bloom that  
19 could be induced within several days, making the *p*CO<sub>2</sub> very difficult to keep under control. Alternatively,  
20 we would have had to dilute 4 tons of seawater in the mesocosm bags at least every two days to maintain  
21 the cell density and CO<sub>2</sub> concentration. Furthermore, considering a number of studies on the typical  
22 phytoplankton responses to OA that have been carried out in laboratory, it was indeed a natural

1 progression for us to use typical model phytoplankton species to initiate the mesocosm studies before  
2 using natural communities. Therefore, using the filtered seawater with inoculated isolates was reasonable  
3 and logistically practical for our experiment.

#### 4 **2.2 Bacteria sampling, filtration and sample selection**

5 A total of 500 mL to 2 L of water, depending on bacterial concentration, was collected from the  
6 mesocosms. Six of the mesocosms (HC: #2, #4, #7 and LC: #1, #6, #8) were chosen for further study.  
7 The inter-replicate variation in mesocosm experiments is usually more significant than in lab  
8 experiments, because mesocosm experiments are conducted in open environments. Initially we had 4  
9 replicates for each treatment, however, mesocosm bag 9 had a hole and mesocosm bag 3 was  
10 contaminated by other phytoplankton in the beginning. Therefore, we did not consider the data from  
11 these two compromised bags. Furthermore, three replicates of each treatment in our experiment to some  
12 extent balanced out the bacteria introduction contingency, although the inter-replicate variation was  
13 significant. Samples from days 4, 6, 8, 10, 13, 19, and 29 were collected in this study due to time,  
14 personnel and equipment constraints. Sequential size fractionated filtration (2  $\mu\text{m}$  and 0.2  $\mu\text{m}$   
15 polycarbonate filters) by peristaltic pump was used to filter seawater collected from the mesocosm bags.  
16 We tried to do sampling at day 2, but the samples were not successfully collected, probably due to very  
17 high concentration of TEP (Transparent Exopolymer Particles) which easily blocked the polycarbonate  
18 filter. Some replicates were missing at day 4 because we were able to successfully extract enough DNA  
19 for sequencing only from bag 1, bag 7 and bag 6, also probably due to high TEP at day 4. It has been  
20 reported that high TEP concentration was associated with high bacteria biomass (Sugimoto et al.,  
21 2007, Ramaiah et al., 2000). According to the bacterioplankton abundance data (Fig. S3, Yibin Huang  
22 et al.), the average bacterioplankton abundance was  $6.69 \times 10^9$  cells/ml and  $9.71 \times 10^9$  cells/ml at day 2



1 and day 4 respectively.

## 2 **2.3 DNA extraction, 16S rDNA V3-V4 region amplification and Illumina MiSeq sequencing**

3 Samples collected by 0.2 µm polycarbonate filters as described above were washed with PBS buffer and  
4 then centrifuged at 9600g to obtain a cell pellet. A previously described DNA extraction protocol  
5 (Francis et al., 2005) was utilized with some modifications, using the columns for DNA purification  
6 from a bacteria DNA extraction kit (Tiangen DP302, China). Amplification, library construction and  
7 sequencing were performed offsite at ANNOROAD using the DNA samples isolated as described above.

8 Primers were 341F (5'-CCTACGGGNGGCWGCAG-3') and 805R  
9 (5'-GACTACHVGGGTATCTAATCC-3'), targeting the V3-V4 hyper variable regions of bacterial 16S  
10 rRNA gene. The PCR amplification condition was as follows: initial denaturation at 95°C for 3 min, 25  
11 cycles of denaturation at 95°C for 30 s, annealing at 55°C for 30 s and extension at 72°C for 30 s, then  
12 final extension at 72°C for 5 min. DNA library construction and sequencing followed the MiSeq Reagent  
13 Kit Preparation Guide (Illumina, USA).

## 14 **2.4 Sequence assignment and sequence statistics analysis**

15 Clean paired-end reads were merged using PEAR (Zhang et al., 2014). The remaining raw sequences  
16 were distinguished and sorted by unique sample tags. Unique operational taxonomic units (OTUs) were  
17 picked against Greengenes database ([http://greengenes.lbl.gov/cgi-bin/JD\\_Tutorial/nph-16S.cgi](http://greengenes.lbl.gov/cgi-bin/JD_Tutorial/nph-16S.cgi))  
18 (McDonald et al., 2012) at 97% identity. OTUs with less than 2 reads were not considered. According to  
19 the reference database, the representative sequences for each OTU were aligned using PyNAST  
20 (Caporaso et al., 2010a). Finally, the phylogenetic tree was generated from the Graphlan (Langille  
21 et al., 2013) using information on both the relative abundance and phylogenetic relationship of  
22 observed species. QIIME 1.8.0 was used for sequence analysis including OTUs extraction for

1 bacterioplankton community structure analysis, OTUs overlapping analysis, species diversity, species  
2 richness analysis and Principal Components Analysis (PCA) (Caporaso et al., 2010b). Bacterioplankton  
3 community composition differences were assessed by Unweighted UniFrac distance using QIIME 1.8.0  
4 as well. Dissimilarity tests were based on the Bray-Curtis dissimilarity index using analysis of  
5 similarities (ANOSIM) (Clarke, 1993), non-parametric multivariate analysis of variance (ADONIS)  
6 (Anderson, 2001), and multi-response permutation procedures (MRPP) (Mielke et al., 1981). Observed  
7 species, Chao index, Shannon index and Simpson index were used for estimating the community  
8 diversity. Analysis of variance (ANOVA) followed by T-test was performed to determine any significant  
9 differences between HC and LC treatments.

## 10 **2.5 Ecological network construction and analysis**

11 As previously described, ecological network construction and analyses were performed based on the  
12 relative abundance of OTUs in HC and LC treatments with three biological replicates  
13 (<http://129.15.40.240/mena/>, Wang et al., 2016). The sequencing data from each mesocosm bag with  
14 time series throughout the experiment were considered as different replicates. First, the similarity  
15 matrices of the relative abundance of OTUs in LC and HC conditions were created respectively using  
16 Pearson correlation coefficient across time points with biological replicates by a random matrix theory  
17 (RMT)-based approach. Cut-off values were determined according to  $R^2$  of power-law larger than 0.8  
18 and equal between two manipulations to construct network structure. In order to ensure the constructed  
19 networks were not random, biologically meaningless networks, 100 networks from the same matrix were  
20 constructed and randomized. This resulted in the experimental networks being different from random  
21 networks judging by significantly higher modularity, clustering coefficient and geodesic distance (Table  
22 1). Then, module separation was produced using greedy modularity optimization, and  $Z-P$  values for all

1 nodes were calculated. In addition, to compare networks, the network connection was randomly rewired  
2 and network topological properties were calculated. Finally, the bacteria network interaction was  
3 visualized by Cytoscape v.3.3.0. The  $Z$ - $P$  plots were constructed based on within-module ( $Z$ ) and  
4 among-module ( $P$ ) values of each node derived from ecological network analysis. Ecological network  
5 analysis is a novel RMT-based framework for studying microbial interactions. A node in ecological  
6 network analysis shows an OTU and a link demonstrates a connection between two OTUs. The shortest  
7 path between nodes is indicated by geodesic distance. Since the network constructed by OTUs can be  
8 separated into several sub-communities, or modules, the modularity value indicates how well a network  
9 can be divided into different sub-communities. Clustering coefficients demonstrate how well an OTU is  
10 connected with other OTUs, while average clustering coefficients indicate the extent of connection in a  
11 network.

## 12 **3 Results**

### 13 **3.1 Environmental parameters and experimental timeline**

14 The initial inorganic nitrogen,  $\text{PO}_4^{3-}$ , and  $\text{SiO}_3^{2-}$  concentrations were 70–75  $\mu\text{mol/L}$ , 2.5–2.6  $\mu\text{mol/L}$ , and  
15 38–39  $\mu\text{mol/L}$ , respectively. Except for  $\text{SiO}_3^{2-}$ , nutrient concentrations decreased with rapid growth of  
16 the phytoplankton and reached low concentrations by day 15. The dissolved total inorganic nitrogen  
17 dropped from an initial concentration of  $74.9 \pm 2.87 \mu\text{mol/L}$  to  $57.2 \pm 4.37 \mu\text{mol/L}$  in the HC condition  
18 and  $72 \pm 5.90 \mu\text{mol/L}$  to  $53.6 \pm 5.60 \mu\text{mol/L}$  in the LC condition by day 8, and reached low  
19 concentrations by day 15 (average  $3 \mu\text{mol/L}$  in LC and average  $6 \mu\text{mol/L}$  in HC ).

20  $\text{pH}_{\text{NBS}}$  was determined on the scene with a pH/mV/ORP Meter (LEAN) calibrated with National  
21 Bureau of Standards (NBS) buffers. Samples for DIC measurement were collected into 250 ml brown  
22 borosilicate glass bottles and poisoned with 250  $\mu\text{L}$  saturated  $\text{HgCl}_2$  solution. DIC was determined by

1 acidification of 0.5 mL samples and subsequently infrared quantification of CO<sub>2</sub> with an Apollo® DIC  
2 Analyzer. pH<sub>total</sub> was determined using a Orion 3 Star pH Benchtop analyzer and a Orion Ross  
3 combined pH electrode, which was calibrated against three NIST-traceable pH buffers (pH 4.01, 7.00  
4 and 10.01) (Cao et al. 2011). The pCO<sub>2</sub> and TA values in this study were calculated from DIC and  
5 pH<sub>total</sub> by the CO2SYS Program (Lewis and Wallace, 1998). The carbonate chemistry data at different  
6 time points are shown in Table S1. A comprehensive description of carbonate chemistry measurements  
7 and analysis during this mesocosm experiment is given in (Yan Li et al, unpublished). The initial pCO<sub>2</sub>  
8 of 373.0 ± 43.9 µatm (pH<sub>NBS</sub>: 8.18 ± 0.02) in the LC treatment and 1296.0 ± 159.6 µatm (pH<sub>NBS</sub>: 7.75 ±  
9 0.04) in the HC treatment increased and reached a peak value of 922.5 ± 142.0 µatm (pH<sub>NBS</sub>: 7.74 ± 0.08)  
10 in the LC treatment at day 8 and 1879.6 ± 145.4 µatm (pH<sub>NBS</sub>: 7.49 ± 0.05) in the HC treatment at day 4.  
11 After reaching the peak, the pCO<sub>2</sub> values of both treatments decreased and were no longer statistically  
12 different from day 13 onwards due to rapid CO<sub>2</sub> uptake by the phytoplankton, despite air containing 1000  
13 ppm CO<sub>2</sub> being continuously bubbled into the HC treatments (Fig. 1 a, b). The bacterioplankton biomass  
14 were very high on day 2 and day 4 (Fig. S3). However, the large amount of DIC (dissolved inorganic  
15 carbon) produced by this high biomass of bacterioplankton could not be consumed by the phytoplankton  
16 which were still at very low biomass, thus explaining the significant DIC production in the beginning.  
17 The continuous rise of pCO<sub>2</sub> until the phytoplankton reached a certain concentration in the beginning was  
18 also due to the high concentration of bacteria and the low concentration of phytoplankton, even though  
19 the seawater was being aerated at target pCO<sub>2</sub>. *P. tricornutum* and *T. weissflogii* were the dominant  
20 species throughout the whole phytoplankton bloom in both HC and LC conditions. Chlorophyll *a* (Chl*a*)  
21 concentration and diatom cell densities were used to identify changes in the diatom bloom following  
22 inoculation (Fig. 1c, Liu et al., 2017). Chl*a* concentration increased from 0.23 ± 0.12 µg/L to 5.33 ± 1.82

1  $\mu\text{g/L}$  in the LC conditions, and from  $0.19 \pm 0.07 \mu\text{g/L}$  to  $5.75 \pm 1.17 \mu\text{g/L}$  in the HC conditions from day  
2 4 to day 9. Thereafter, *Chla* concentration increased significantly and peaked at  $109.9 \pm 38.04 \mu\text{g/L}$  in the  
3 LC treatment and  $108.6 \pm 46.07 \mu\text{g/L}$  in the HC treatment at day 15. Subsequently, *Chla* concentrations  
4 in both treatments were maintained at high concentrations until day 25 and decreased progressively  
5 afterward. The bloom process identified by cell concentration of *P. tricornutum* and *T. weissflogii* was  
6 similar with that illustrated by *Chla* concentration. The growth of these two diatom species entered into  
7 logarithmic phase from day 2. Cell density reached highest concentration at day 15 and day 19 for *T.*  
8 *weissflogii* and *P. tricornutum* respectively, and then dropped down slowly. The coccolithophore  
9 *Emiliana huxleyi* largely disappeared from the experimental mesocosms. A comprehensive description  
10 of phytoplankton cell density, *Chla* concentration, particle organic carbon (POC) and particle organic  
11 nitrogen (PON) during the experiment is given in (Liu et al., 2017).

### 12 **3.2 Overview of sequencing analysis**

13 Following sequencing, 828524 high quality sequences were kept after processing (Table. S2), and 39.3%  
14 of assembled reads were successfully aligned with the database. As a result, a total of unique 557  
15 OTUs were generated after clustering at a 97% similarity level. 49.1% of OTUs were classified to  
16 genera level with high taxonomic resolution (Table. S3). The phylogenetic tree was constructed based on  
17 the sequences derived from all of the samples (Fig. S4). The bacterioplankton from all of the samples in  
18 this study were identified as members of Bacteroidetes or Proteobacteria phylums. The most dominant  
19 OTUs were Alphaproteobacteria, Rhodobacterales, Rhodobacterceae and Sediminicola at class, order,  
20 family and genus level respectively (Fig. S5). The most abundant sequences at class, order, family and  
21 genus levels accounted for 43.4 %, 42.6 %, 41.7% and 32.8 % of all sequences respectively.

### 1 **3.3 Bacterioplankton community structure throughout the phytoplankton bloom**

2 The bacterioplankton community structure in the mesocosm bags was very different from that in the  
3 originally inoculated phytoplankton cultures by day 4. For instance, some bacterioplankton phyla not  
4 detected in the original phytoplankton culture were observed in the samples collected on day 4. This  
5 may indicate that the bacterioplankton from the natural environment gradually became dominant in the  
6 mesocosm bags from day 0 to day 4. For example, Epsilonbacteria appeared in the mesocosms at day 4,  
7 while no Epsilonbacteria were detected in the coccolithophore or diatom cultures. Nearly 50% of the  
8 bacterioplankton in the mesocosms were composed of Epsilonbacteria in D4.1 (Fig. S2, Fig. 2).

9 Bacterioplankton community structure underwent dynamic changes during the diatom bloom in both  
10 the HC and LC treatments, varying significantly at different stages of the phytoplankton bloom (Fig. 2).  
11 At the phylum level, the bacterioplankton were dominated by Proteobacteria, while the relative  
12 abundance of Bacteroidetes was very low when nutrients were replete and diatom biomass was not high.  
13 However, Bacteroidetes increased dramatically as diatom biomass increased, and began to drop down  
14 after reaching a peak at day 10 (Fig. 2 and Fig. 3). In contrast, Proteobacteria began to increase after  
15 reaching their lowest concentration at day 10.

16 The Alphaproteobacteria, Flavobacteria, and Gammaproteobacteria classes with high abundance in all  
17 samples were selected for further analysis. The proportion of the Gammaproteobacteria class from the  
18 Proteobacteria phylum was very high at the beginning of the experiment ( $50.2 \pm 13.8$  % in the HC  
19 treatment and  $44.1 \pm 6.4$  % in the LC treatment at day 6) and decreased throughout the duration of the  
20 experiment. On the other hand, the Alphaproteobacteria class, also from the Proteobacteria phylum,  
21 decreased from initially high proportions ( $46.9 \pm 13.2$  % in the HC treatment and  $43.9 \pm 11.6$  % in the LC  
22 treatment) at day 6 to low proportions at day 10 ( $27.2 \pm 2.8$  %) in the HC treatment, but remained almost

1 unchanged ( $44.6 \pm 7.5$  %) in the LC treatment and increased to  $63.2 \pm 27.3$  % in the HC treatment and  
2  $60.8 \pm 32.7$  % in the LC treatment at day 29 (Fig. 2 and Fig. 3). The relative abundance of the  
3 Flavobacteria class from the Bacteroidetes increased from the beginning and reached a peak at day 10  
4 ( $52.2 \pm 4.2$  % in the HC treatment and  $24.8 \pm 16.9$  % in the LC treatment), then dropped down until day  
5 19 ( $19.9 \pm 2.2$  % in the HC treatment and  $18.0 \pm 15.4$ % in the LC treatment) (Fig. 2 and Fig. 3). The  
6 proportional variation of the Flavobacteriales order and the Rhodobacterales order showed similar trends  
7 with the Flavobacteria class and the Alphaproteobacteria class, respectively, as shown in Fig. 2 and Fig.  
8 3.

#### 9 **3.4 The effects of elevated CO<sub>2</sub> on bacterioplankton community structure**

10 Bacterial community structures of the HC and LC treatments were compared at different sampling  
11 time-points (Fig 2), and a dissimilarity test based on ANOSIM, MRPP and ADONIS methods showed  
12 that no statistically significant differences were observed (Table 2). PCA analysis also agreed with the  
13 dissimilarity test (Fig. S8). The bacterioplankton community diversity in all samples was estimated by  
14 observed species, Chao index, Shannon index and Simpson index. Rarefaction curves showed no  
15 remarkable differences in community diversity between HC and LC, regardless of the time point (Fig.  
16 S6). In general, bacterioplankton community diversity in both HC and LC treatments followed the same  
17 trend, in that it peaked at day 10 and declined for the remainder of the experiment (Fig. S7).

18 Although the general trend of bacterioplankton community structure variation was similar in both the  
19 HC and LC treatments as described above, some groups of bacterioplankton showed different responses  
20 to elevated CO<sub>2</sub> at some time points. Notably, Bacteroidetes (predominantly Flavobacteria) had a higher  
21 average proportion in the HC treatment ( $52.2$  % of Bacteroidetes and  $52.2$  % of Flavobacteria) than in the  
22 LC treatment ( $25.2$ % Bacteroidetes and  $24.8$ % Flavobacteria) at the early stage of the diatom bloom at

1 day 10 ( $p=0.049$  and  $0.053$  respectively). In contrast Proteobacteria, especially the Alphaproteobacteria,  
2 were observed to have lower proportion in the HC treatment (47.8 % of Proteobacteria and 27.2% of  
3 Alphaproteobacteria) than in the LC treatment (74.8 % of Proteobacteria and 44.6% of  
4 Alphaproteobacteria) at day 10 ( $p=0.049$  and  $0.019$  respectively, Fig. 3). At a higher taxonomic level,  
5 Flavobacteriales demonstrated higher relative abundance in the HC treatment (52.2 %) compared to the  
6 LC treatment (24.8 %) at day 10 ( $p=0.053$ ), while for Rhodobacterales the inverse pattern was observed  
7 ( $p=0.020$ ). Moreover, Flavobacteriaceae were observed to have a relatively higher ratio in the HC  
8 treatment (50.3 %) compared to the LC treatment (24.0 %) at day 10 ( $p=0.053$ ), whereas  
9 Rhodobacteraceae demonstrated the opposite pattern ( $p=0.021$ , Fig. 3). It is notable that  
10 Alteromonadales, belonging to the Gammaproteobacteria, had a higher ratio in the HC treatment  
11 compared to the LC treatment at day 19 and day 29, although this was not statistically significant ( $p=0.24$   
12 and  $0.34$  at day 19 and 29 respectively).

### 13 **3.5 The effects of elevated CO<sub>2</sub> on bacterioplankton community interactions**

14 Both HC and LC networks were dominated by Alphaproteobacteria, Gammaproteobacteria and  
15 Flavobacteria, suggesting their vital roles in maintaining stability of microbial ecosystems under both  
16 HC and LC conditions. The observation of more negative links compared to positive links indicates the  
17 dominant relationship among bacterioplankton is competitive rather than mutualistic under both the HC  
18 and LC treatments. The average connectivity and clustering coefficient of the network were higher in the  
19 HC treatment than in the LC treatment, while geodesic distance and modularity value was higher in the  
20 the LC treatment. Bacterioplankton formed more modules under the LC treatment, but were densely  
21 connected in less modules under the HC treatment (Table 1, Fig. 4). However, as shown in Fig. 4, the  
22 links among the OTUs with high abundance, 558885 (Rhodobacteraceae), 572670 (Rhodobacteraceae),



1 190052 (Flavobacteriaceae), 107130 (Flavobacteriaceae) and 4331023 (Rhodobacteraceae), were  
2 positive in both HC and LC.

3 Interestingly, some nodes that were sparsely distributed in independent modules in the LC network  
4 formed dense modules with high connectivity in the HC network (Fig. 4). As the OTUs connected within  
5 a module, they could be considered as a putative bacterioplankton ecological niche (Zhou et al., 2010). It  
6 is plausible that elevated CO<sub>2</sub> disrupted the connection between different bacterioplankton community  
7 niches, but enhanced alternative connections among species within certain ecological niches. Within  
8 module connectivity (*Zi*) and among-module connectivity (*Pi*) indexes were used to identify key module  
9 members (Olesen et al., 2007, Fig. 5). In an ecological context, the peripherals may represent specialists,  
10 while module hubs and connectors may be considered more as intra-module and inter-module generalists  
11 respectively. Network hubs are usually considered as super-generalists (Deng et al., 2012). It is  
12 interesting that the numbers of connectors that are considered as generalists were reduced, whereas  
13 module hubs were increased under the HC treatment. However, two network hubs, the super-generalists  
14 that are more important than module hubs and connectors, were detected in the LC network but not in the  
15 HC network (Fig. 5).

#### 16 **4 Discussion**

17 This study was designed to bridge the gap between lab cultures and field studies, with isolates of  
18 non-axenic phytoplankton being added to filtered natural waters. The lab conditions possibly have  
19 selected for a fast-growing bacterial community adapted to live with semi-continuous phytoplankton  
20 culture. Therefore, the inoculated bacterioplankton were likely preconditioned to lab conditions in  
21 semi-continuous phytoplankton cultures prior to the experiment. However, the bacterioplankton from  
22 the natural environment gradually became dominant in the mesocosm bags from day 0 to day 4, based

1 on the comparison of the community at day 4 and the original community in the phytoplankton cultures.  
2 For instance, during these 4 days members of the *Arcobacter* genus (OTU 553961) and  
3 *Pseudomonadaceae* family (OUT 543958) were introduced from surrounding seawater into the  
4 mesocosm bags. The bacterial growth rates under eutrophic conditions are much higher than under  
5 oligotrophic conditions (White et al., 1991; Kirchman, 2016). The bacterial growth rate reached 16.2  
6  $\text{day}^{-1}$  ( $0.675 \text{ h}^{-1}$ ) during a diatom bloom in a mesocosm experiment using seawater from Santa Barbara  
7 Channel amended with nutrients (Smith et al., 1995). Under simulated eutrophication conditions, the  
8 growth rates of bacteria from the Mediterranean sea ranged from  $0.245 \text{ h}^{-1}$  to  $0.853 \text{ h}^{-1}$  based on the  
9 data measured roughly every 24 hours in batch mesocosms (Lebaron et al., 1999). We would like to  
10 point out that our experiments were conducted in eutrophic coastal seawaters with reduced predatory  
11 grazing pressure due to seawater filtration, which could stimulate the net bacterial growth rate. In  
12 addition, some species belong to *Pseudomonas* group, one of the most abundant bacterioplankton group  
13 from outside, were reported to have high growth rates (Adav, 2008; Eagon, 1962). Therefore, we think  
14 choosing  $0.5 \text{ h}^{-1}$  as the bacterial growth rate of the bacterioplankton is tenable. In our study, assuming  
15 the bacterioplankton concentration at day 2 representing the concentration of *Pseudomonadaceae*, one  
16 of the most abundant bacterioplankton groups from surrounding seawater, the concentration of  
17 *Pseudomonadaceae* at day 0 could be estimated based on the growth rate of  $0.5 \text{ h}^{-1}$  and the  
18 bacterioplankton concentration ( $6.693 \times 10^9$  cells/ml) at day 2. The estimated concentration of  
19 *Pseudomonadaceae* at day 0 was about 3 cells/ml. Therefore, the ratio of bacteria being continuously  
20 introduced to actual standing stocks in the mesocosms was low, which allowed us to detect potential  
21  $\text{CO}_2$  effects in this mesocosm experiment.

22 The seawater used in this mesocosm experiment was filtered natural seawater (through  $0.01 \mu\text{m}$  filter)

1 in Wuyuan bay. Although no bacteria or phytoplankton were detected in the filtered seawater by flow  
2 cytometry, high concentrations of DOM (dissolved organic matter) and other nutrients in the seawater  
3 could not be filtered out. According to Yan Li et al (unpublished), the dissolved organic carbon (DOC)  
4 concentration was 258.9  $\mu\text{mol/L}$  in average at day 2. It was not surprising that bacterioplankton were  
5 able to grow very quickly with such high concentrations of DOC. Because the  
6 phytoplankton-associated bacterioplankton were presumably adapted to the phytoplankton cultures,  
7 they were used to living in the artificial seawater, not the local seawater in Wuyuan Bay. As the local  
8 bacterioplankton were presumably well adapted to local conditions (such as high DOC concentration)  
9 in Wuyuan Bay, it is perhaps not surprising that they could easily outcompete the phytoplankton  
10 culture-derived bacterioplankton. Although bacterioplankton from the phytoplankton cultures were  
11 inoculated into the mesocosm system at the beginning of the experiment, they were mostly replaced by  
12 the natural bacterioplankton community within several days. Therefore, the natural bacterioplankton,  
13 not the original bacterioplankton from the phytoplankton culture, mainly determined the final responses  
14 of the community to different  $\text{CO}_2$  concentrations.

15 In this mesocosm experiment, significant variation in community structure was observed through the  
16 whole diatom bloom process, suggesting that the diatom bloom was a major driver for bacterioplankton  
17 community structure dynamics in both the HC and LC treatments. This finding is in line with previous  
18 mesocosm experiments and field observations (Allgaier et al., 2008, Teeling et al., 2012). Along with  
19 the phytoplankton bloom process, the inter-replicate variation of bacterioplankton community became  
20 more apparent, which was inevitable for an outdoor mesocosm experiment. For example, the  
21 bacterioplankton community in mesocosm bag 8 was dominated by *Phaeobacter. sp* at day 29, which  
22 was distinct from the other mesocosm bags. According to the phytoplankton data mesocosm bag 8 was

1 probably contaminated with dinoflagellates at a late stage of the algal bloom, likely resulting in a  
2 different bacterioplankton community structure compared to the others. In general, no statistically  
3 significant differences were detected in this study, probably due to high variability among replicates. At  
4 day 10 the inter-replicate-variability in the relative abundance of some groups of bacterioplankton was  
5 relatively low, especially for the HC treatment. Indeed, statistically significant differences between the  
6 HC and LC treatments in the abundances of certain groups of bacterioplankton were detected at day 10.  
7 Therefore, only when the variability among replicates was smaller than the variability between  
8 different treatments could statistically differences between treatments be detected.

9     Although effects of elevated CO<sub>2</sub> on bacterioplankton communities have been reported (Allgaier et al.,  
10 2008; Tanaka et al., 2008; Wang et al., 2016; Zhang et al., 2013; Ray et al., 2012; Roy et al., 2013;  
11 Baltar et al., 2015; reviewed in Hutchins and Fu, 2017), how marine bacteria communities react to the  
12 occurrence of elevated CO<sub>2</sub> in eutrophic seawater is still uncertain. This mesocosm study  
13 comprehensively investigated the effects of elevated CO<sub>2</sub> on bacterioplankton community structure and  
14 networks using Illumina sequencing and ecological network analysis in the context of eutrophication.  
15 Compared to the effects of the phytoplankton bloom, ocean acidification did not strongly influence the  
16 bacterioplankton community structure. The results indicate that bacterial abundance and community  
17 structure at different taxonomic levels were generally similar between the HC and LC treatments at the  
18 different diatom bloom stages, in line with previous ocean acidification mesocosm bacterioplankton  
19 community studies (Tanaka et al., 2008; Wang et al., 2016; Zhang et al., 2013; Ray et al., 2012; Roy et  
20 al., 2013; Baltar et al., 2015). Differences in bacterioplankton community diversity between the HC and  
21 LC treatments were also not remarkable. These results suggest the possibility that the whole  
22 bacterioplankton community has a certain degree of resilience to elevated CO<sub>2</sub>, which is consistent with

1 a previous stated hypothesis (Joint et al., 2011).

2 It has previously been proposed that the observed insignificant effects of ocean acidification on coastal  
3 bacterioplankton may be due to their adaptation to strong natural variability in pH in coastal ecosystems,  
4 where amplitudes of >0.3 units from diel fluctuations and seasonal dynamics are commonly seen  
5 (Hofmann et al., 2011). The comparative ecological network analysis in this study to some extent  
6 explains the resilience of the bacterioplankton community to elevated CO<sub>2</sub> levels. According to the  
7 present study, substantial numbers of OTUs that were sparsely distributed in different and small modules  
8 in the LC network became connected with each other and formed fewer modules in the HC network,  
9 implying elevated CO<sub>2</sub> has the potential to reassemble the bacterioplankton community (Fig. 4). The  
10 positive relationship among these principal components were almost unaltered in the network analysis,  
11 suggesting that the positive relationships among them were robust in the face of CO<sub>2</sub> changes, thus  
12 contributing to whole community stability (Fig. 4). It has also been reported that sparsely distributed  
13 fungal species were reassembled into highly connected dense modules under long-term elevated CO<sub>2</sub>  
14 conditions (Tu et al., 2015).

15 It is noteworthy that the OTUs involved in possible community reassembly were not very abundant,  
16 whereas the relationship between the abundant OTUs was virtually unaltered by elevated CO<sub>2</sub> in this  
17 study. Although elevated CO<sub>2</sub> promoted the reassembly of the bacterioplankton community, the network  
18 constructed by abundant OTUs which are usually considered as the foundation of the whole  
19 bacterioplankton community was still stable in response to elevated CO<sub>2</sub>. This to some extent led to  
20 maintenance of bacterioplankton community structure under the ocean acidification stimuli in the  
21 context of eutrophic conditions. Additionally, these data indicate that more negative than positive  
22 relationships between OTUs were observed in both HC and LC treatments, which is consistent with a

1 previous ocean acidification mesocosm study conducted in the Arctic Ocean (Wang et al., 2016). It was  
2 proposed that a community with more competitors would be more stable and yield less variation under  
3 environmental fluctuations (Gonzalez and Loreau, 2009). Therefore, it could be speculated that the  
4 dominant competitive relationship between bacterioplankton species in this mesocosm experiment  
5 helped the whole bacterioplankton community to adapt to pH perturbations, with less variation in total  
6 biomass and diversity.

7 Although the effects of elevated CO<sub>2</sub> on bacterioplankton community structure were not significant,  
8 the proportion of some groups of bacterioplankton varied between the HC and LC treatments in the early  
9 stages of the diatom bloom. Elevated CO<sub>2</sub> significantly increased the proportion of Flavobacteria  
10 (dominated by Flavobacteriales) in the HC treatment at day 10, when the diatoms cells began to grow  
11 rapidly. In contrast, the HC treatment had negative effects on the growth of Alphaproteobacteria  
12 compared to the LC treatment. The results reported here are in line with previous reports about the  
13 response of Flavobacteria to ocean acidification in biofilm and single species experiments (Witt et al.,  
14 2011; Teira et al., 2012). Flavobacteria are considered as the “first responders” to phytoplankton blooms  
15 because they specialize in attacking algal cells and further degrading biopolymers and organic matter  
16 derived from algal detrital particles (Kirchman, 2002; Teeling et al., 2012). Flavobacteria are especially  
17 good at converting high molecular weight (HMW) dissolved organic matter (DOM) to low molecular  
18 weight (LMW) DOM using the highly efficient, extracellular, multi-protein complex TonB-dependent  
19 transporter (TBDT) system, based on previous in situ proteomics and metatranscriptomics data (Teeling  
20 et al., 2012). Higher abundance of Flavobacteria under elevated CO<sub>2</sub> means more HMW DOM could be  
21 degraded and so enter into the carbon cycle (Buchan et al., 2014). Based on the results reported here, it  
22 can be speculated that increased amounts of Flavobacteria under the elevated CO<sub>2</sub> treatment in eutrophic

1 seawater could promote the TBDT system to break down HMW DOM and lead to improved efficiency  
2 of the Microbial Carbon Pump (MCP), and possibly further influence the carbon storage in the ocean  
3 (Jiao et al., 2010). It has also been postulated that the Flavobacteria-originated, light-driven proton pump  
4 proteorhodopsin could be involved in dealing with ocean acidification and pH perturbation (Fuhrman et  
5 al., 2008). Recent metatranscriptomic data further emphasize the role of proteorhodopsin in pH  
6 homeostasis in bacterioplankton under elevated CO<sub>2</sub> (Bunse et al., 2016; Gómez-Consarnau et al., 2007).  
7 The underlying mechanisms underlying the enhanced growth of Flavobacteria under elevated CO<sub>2</sub> need  
8 further investigation in the future.

9 Interestingly, Flavobacteria in our study showed higher abundance in the HC treatment in the early  
10 phytoplankton bloom stage. However, a negative relationship between CO<sub>2</sub> level and relative abundance  
11 of Bacteroidetes based on terminal restriction fragment length polymorphism (T-RFLP) method was  
12 observed in a mesocosm experiment conducted in the Arctic region with low nutrient levels (Roy et al.,  
13 2013). Moreover, the effects of elevated CO<sub>2</sub> on bacterioplankton community interaction webs in this  
14 study were not observed in previous mesocosm work in the Arctic Ocean (Wang et al., 2016; Roy et al.,  
15 2013). The results of the current study showed that the effects of elevated CO<sub>2</sub> in the context of  
16 eutrophication were different compared to elevated CO<sub>2</sub> on bacterioplankton community networks in a  
17 mesocosm study carried out in the oligotrophic Arctic Ocean. The data here and previously reported,  
18 seemingly contradictory results highlight the importance of including the combined effects of ocean  
19 acidification and other anthropogenic perturbations to interpret and predict the impact of global change  
20 on marine life.

21 In this study, the majority of the particle-attached and algae-attached bacteria were filtered out by  
22 sequential filtering. Additionally, the archaea were not included in our data because we used the

1 primers 341F/805R, which do not target archaea. Therefore, the community structure of  
2 particle-associated bacteria and all archaea were not investigated in our study. Furthermore, a  
3 simplified model phytoplankton community was used in this study, composed of the two diatom species  
4 *P. tricornutum* and *T. weissflogii* in both LC and HC treatments. It is possible that the similarity of the  
5 two bacterial communities in the two treatments was due to the similar composition and quality of DOM  
6 produced by these two diatoms. With a more diverse natural phytoplankton community experimental  
7 system, perhaps different phytoplankton taxa would have dominated in the HC and LC treatments,  
8 leading to different bacterial communities. In future studies, it would also be worthwhile to sample over  
9 a diel cycle in order to understand the cyclic variability in pH, and whether this affects short term changes  
10 in bacterioplankton community structure.

## 11 **Conclusion**

12 Elevated CO<sub>2</sub> was not a strong influence on bacterioplankton community structure compared to the  
13 diatom bloom process, based on 16S V3-V4 region Illumina sequencing. Based on ecological network  
14 analysis, elevated CO<sub>2</sub> appeared to reassemble the community network of taxa present with low  
15 abundance, but barely altered the network structure of the bacterioplankton taxa present with high  
16 abundance. It is this differential sensitivity of common and rare groups to carbonate chemistry changes  
17 that may largely explain the resilience of the bacterioplankton community to elevated CO<sub>2</sub>.

## 18 **Author contributions**

19 Conceived and designed the experiments: K. Gao, X. Lin, M. Dai. Performed the experiments: R. Huang,  
20 X. Lin, Y. Wu, Y. Li and F. Li. Analysed data: R. Huang and X. Lin. Wrote the paper: X. Lin. Revised  
21 the paper: D. Hutchins and K. Gao. All authors reviewed the manuscript.



1 **Acknowledgments**

2 This study was supported by the National Key Research and Development Program of China (Grant No.  
3 2016YFA0601302), the National Natural Science Foundation of China (No. 41306096 to X. Lin, No.  
4 41430967 and No. 41120164007 to K. Gao), State Oceanic Administration of China  
5 (SOA,GASI-03-01-02-04), The Open Fund of Key Laboratory of Marine Ecology and Environmental  
6 Sciences, Institute of Oceanology, Chinese Academy of Sciences, and Laboratory of Marine Ecology  
7 and Environmental Science, Qingdao National Laboratory for Marine Science and Technology  
8 (KLMEES201608), Joint project of NSFC and Shandong province (Grant No. U1406403), Strategic  
9 Priority Research Program of Chinese Academy of Sciences (Grant No. XDA11020302). DAH's  
10 contributions were supported by U.S. NSF OCE 1260490 and 1538525, and his visits to Xiamen were  
11 supported by "111" project from the Ministry of Education. We thank X. Liu, T. Xing, X. Cai, N. Liu, S.  
12 Tong, X. Yi, T. Wang, H. Miao, Z. Li, D. Yan, W. Zhao and X. Zeng for their kind assistance in  
13 operations of the mesocosm experiment.

14 **Competing interests:**

15 The authors declare no competing financial interests.

16 **Reference**

17 Allgaier, M., Riebesell, U., Vogt, M., Thyrrhaug, R. and Grossart, H.-P.: Coupling of heterotrophic  
18 bacteria to phytoplankton bloom development at different pCO<sub>2</sub> levels: a mesocosm study,  
19 Biogeosciences, 5(4), 1007–1022, doi:10.5194/bgd-5-317-2008, 2008.  
20 Anderson, M. J.: A new method for non-parametric multivariate analysis of variance, Austral Ecol.,  
21 26(2001), 32–46, doi:10.1046/j.1442-9993.2001.01070.x, 2001.

1 Adav, S. S. and Lee, D. J.: Physiological characterization and interactions of isolates in  
2 phenol-degrading aerobic granules, *Appl. Microbiol. Biotechnol.*, 78(5), 899–905,  
3 doi:10.1007/s00253-008-1370-0, 2008.

4 Azam, F.: Microbial control of oceanic carbon flux: the plot thickens., *Science* (80-. ), 280(5364),  
5 694–696, doi:10.1126/science.280.5364.694, 1998.

6 Baltar, F., Palovaara, J., Vila-Costa, M., Salazar, G., Calvo, E., Pelejero, C., Marrasé, C., Gasol, J. M.  
7 and Pinhassil, J.: Response of rare, common and abundant bacterioplankton to anthropogenic  
8 perturbations in a Mediterranean coastal site, *FEMS Microbiol. Ecol.*, 91(6), 1–12,  
9 doi:10.1093/femsec/fiv058, 2015.

10 Buchan, A., LeCleir, G. R., Gulvik, C. A. and González, J. M.: Master recyclers: features and functions  
11 of bacteria associated with phytoplankton blooms, *Nat. Rev. Microbiol.*, 12(10), 686–698,  
12 doi:10.1038/nrmicro3326, 2014.

13 Bunse, C., Lundin, D., Karlsson, C. M. G., Vila-Costa, M., Palovaara, J., Akram, N., Svensson, L.,  
14 Holmfeldt, K., González, J. M., Calvo, E., Pelejero, C., Marrasé, C., Dopson, M., Gasol, J. M. and  
15 Pinhassi, J.: Response of marine bacterioplankton pH homeostasis gene expression to elevated CO<sub>2</sub>,  
16 *Nat. Clim. Chang.*, (January), doi:10.1038/nclimate2914, 2016.

17 Busch, D. S., O'Donnell, M. J., Hauri, C., Mach, K. J., Poach, M., Doney, S. C. and Signorini, S. R.:  
18 Understanding, characterizing, and communicating responses to ocean acidification: Challenges and  
19 uncertainties, *Oceanography*, 28(2), 30–39, doi:http://dx.doi.org/10.5670/oceanog.2015.29, 2015.

20 Cai, W.-J., Hu, X., Huang, W.-J., Murrell, M. C., Lehrter, J. C., Lohrenz, S. E., Chou, W.-C., Zhai, W.,  
21 Hollibaugh, J. T., Wang, Y., Zhao, P., Guo, X., Gundersen, K., Dai, M. and Gong, G.-C.: Acidification  
22 of subsurface coastal waters enhanced by eutrophication, *Nat. Geosci.*, 4(11), 766–770,

1 doi:10.1038/ngeo1297, 2011.

2 Cao, Z., Dai, M., Zheng, N., Wang, D., Li, Q., Zhai, W., Meng, F. and Gan J.: Dynamics of the  
3 carbonate system in a large continental shelf system under the influence of both a river plume and  
4 coastal upwelling, *Journal of Geophysical Research: Biogeosciences*, 116(G2): 582-593, doi:  
5 10.1029/2010jg001596, 2011

6 Caporaso, J. G., Kuczynski, J., Stombaugh, J., Bittinger, K., Bushman, F. D., Costello, E. K., Fierer, N.,  
7 Peña, A. G., Goodrich, J. K., Gordon, J. I., Huttley, G. a, Kelley, S. T., Knights, D., Koenig, J. E., Ley,  
8 R. E., Lozupone, C. a, Mcdonald, D., Muegge, B. D., Pirrung, M., Reeder, J., Sevinsky, J. R.,  
9 Turnbaugh, P. J., Walters, W. a, Widmann, J., Yatsunenko, T., Zaneveld, J. and Knight, R.:  
10 correspondence QIIME allows analysis of high- throughput community sequencing data Intensity  
11 normalization improves color calling in SOLiD sequencing, *Nat. Publ. Gr.*, 7(5), 335–336,  
12 doi:10.1038/nmeth0510-335, 2010a.

13 Caporaso, J. G., Bittinger, K., Bushman, F. D., Desantis, T. Z., Andersen, G. L. and Knight, R.:  
14 PyNAST: A flexible tool for aligning sequences to a template alignment, *Bioinformatics*, 26(2), 266–  
15 267, doi:10.1093/bioinformatics/btp636, 2010b.

16 Clarke, K. R.: Non-parametric multivariate analyses of changes in community, *Aust. J. Ecol.*, 18(1),  
17 117–143, doi:10.1111/j.1442-9993.1993.tb00438.x, 1993.

18 Deng, Y., Jiang, Y.-H., Yang, Y., He, Z., Luo, F. and Zhou, J.: Molecular ecological network analyses,  
19 *BMC Bioinformatics*, 13, 113, doi:10.1186/1471-2105-13-113, 2012.

20 Eagon, R. G.: *Pseudomonas natriegens*, a marine bacterium with a generation, *J. Bacteriol.*, 83(4), 736–  
21 737, 1962.

22 Falkowski, P. G., Fenchel, T. and Delong, E. F.: The Microbial Engines That Drive Earth's

1 Biogeochemical Cycles, *Science* (80-. ), 320(5879), 1034–1039, doi:10.1126/science.1153213, 2008.

2 Francis, C. A., Roberts, K. J., Beman, J. M., Santoro, A. E. and Oakley, B. B.: Ubiquity and diversity  
3 of ammonia-oxidizing archaea in water columns and sediments of the ocean, , 102(41), 14683–14688,  
4 doi:10.1073/pnas.0506625102, 2005.

5 Fuhrman, J. a, Schwalbach, M. S. and Stingl, U.: Proteorhodopsins: an array of physiological roles?,  
6 *Nat. Rev. Microbiol.*, 6(6), 488–494, doi:10.1038/nrmicro1893, 2008.

7 Gattuso, J.-P., Magnan, A., Bille, R., Cheung, W. W. L., Howes, E. L., Joos, F., Allemand, D., Bopp,  
8 L., Cooley, S. R., Eakin, C. M., Hoegh-Guldberg, O., Kelly, R. P., Portner, H.-O., Rogers, a. D.,  
9 Baxter, J. M., Laffoley, D., Osborn, D., Rankovic, A., Rochette, J., Sumaila, U. R., Treyer, S. and  
10 Turley, C.: Contrasting futures for ocean and society from different anthropogenic CO2 emissions  
11 scenarios, *Science* (80-. ), 349(6243), aac4722-1-aac4722-10, doi:10.1126/science.aac4722, 2015.

12 Gómez-Consarnau, L., González, J. M., Coll-Lladó, M., Gourdon, P., Pascher, T., Neutze, R.,  
13 Pedrós-Alió, C. and Pinhassi, J.: Light stimulates growth of proteorhodopsin-containing marine  
14 Flavobacteria, *Nature*, 445(7124), 210–213, doi:10.1038/nature05381, 2007.

15 Gonzalez, A. and Loreau, M.: The Causes and Consequences of Compensatory Dynamics in Ecological  
16 Communities, *Annu. Rev. Ecol. Evol. Syst.*, 40(1), 393–414,  
17 doi:10.1146/annurev.ecolsys.39.110707.173349, 2009.

18 Guidi, L., Chaffron, S., Bittner, L., Eveillard, D., Larhlimi, A., Roux, S., Darzi, Y., Audic, S., Berline,  
19 L., Brum, J., Coelho, L. P., Espinoza, J. C. I., Malviya, S., Sunagawa, S., Dimier, C., Kandels-Lewis, S.,  
20 Picheral, M., Poulain, J., Searson, S., Coordinators, T. O., Stemmann, L., Not, F., Hingamp, P., Speich,  
21 S., Follows, M., Karp-Boss, L., Boss, E., Ogata, H., Pesant, S., Weissenbach, J., Wincker, P., Acinas, S.  
22 G., Bork, P., de Vargas, C., Iudicone, D., Sullivan, M. B., Raes, J., Karsenti, E., Bowler, C. and Gorsky,

1 G.: Plankton networks driving carbon export in the oligotrophic ocean, *Nature*, 532(7600),  
2 doi:10.1038/nature16942, 2016.

3 Hofmann, G. E., Smith, J. E., Johnson, K. S., Send, U., Levin, L. A., Micheli, F., Paytan, A., Price, N.  
4 N., Peterson, B., Takeshita, Y., Matson, P. G., Crook, E. D., Kroeker, K. J., Gambi, M. C., Rivest, E. B.,  
5 Frieder, C. A., Yu, P. C. and Martz, T. R.: High-Frequency Dynamics of Ocean pH: A  
6 Multi-Ecosystem Comparison, *PLoS One*, 6(12), e28983, doi:10.1371/journal.pone.0028983, 2011.

7 Hutchins, D. A. and Fu, F.: Microorganisms and ocean global change, *Nat. Microbiol.*, 2(6), 17058,  
8 doi:10.1038/nmicrobiol.2017.58, 2017.

9 Jiao, N., Herndl, G. J., Hansell, D. A., Benner, R., Kattner, G., Wilhelm, S. W., Kirchman, D. L.,  
10 Weinbauer, M. G., Luo, T., Chen, F. and Azam, F.: Microbial production of recalcitrant dissolved  
11 organic matter: long-term carbon storage in the global ocean, *Nat. Rev. Microbiol.*, 8(8), 593–599,  
12 doi:10.1038/nrmicro2386, 2010.

13 Jin, P., Wang, T., Liu, N., Dupont, S., Beardall, J., Boyd, P. W., Riebesell, U. and Gao, K.: Ocean  
14 acidification increases the accumulation of toxic phenolic compounds across trophic levels., *Nat.*  
15 *Commun.*, 6(October), 8714, doi:10.1038/ncomms9714, 2015.

16 Joint, I., Doney, S. C. and Karl, D. M.: Will ocean acidification affect marine microbes?, *ISME J.*, 5(1),  
17 1–7, doi:10.1038/ismej.2010.79, 2011.

18 Kirchman, D. L.: The ecology of Cytophaga-Flavobacteria in aquatic environments, *FEMS Microbiol.*  
19 *Ecol.*, 39(2), 91–100, doi:10.1016/S0168-6496(01)00206-9, 2002.

20 Kirchman, D. L.: Growth Rates of Microbes in the Oceans, *Ann. Rev. Mar. Sci.*, 8(1), 285–309,  
21 doi:10.1146/annurev-marine-122414-033938, 2016.

22 Krause, E., Wichels, A., Giménez, L., Lunau, M., Schilhabel, M. B. and Gerdtts, G.: Small Changes in

1 pH Have Direct Effects on Marine Bacterial Community Composition: A Microcosm Approach, *PLoS*  
2 *One*, 7(10), e47035, doi:10.1371/journal.pone.0047035, 2012.

3 Labare, M. P., Bays, J. T., Butkus, M. a., Snyder-Leiby, T., Smith, A., Goldstein, A., Schwartz, J. D.,  
4 Wilson, K. C., Ginter, M. R., Bare, E. a., Watts, R. E., Michealson, E., Miller, N. and LaBranche, R.:  
5 The effects of elevated carbon dioxide levels on a *Vibrio* sp. isolated from the deep-sea, *Environ. Sci.*  
6 *Pollut. Res.*, 17(4), 1009–1015, doi:10.1007/s11356-010-0297-z, 2010.

7 Langille, M., Zaneveld, J., Caporaso, J. G., McDonald, D., Knights, D., Reyes, J., Clemente, J.,  
8 Burkepile, D., Vega Thurber, R., Knight, R., Beiko, R. and Huttenhower, C.: Predictive functional  
9 profiling of microbial communities using 16S rRNA marker gene sequences., *Nat. Biotechnol.*, 31(9),  
10 814–21, doi:10.1038/nbt.2676, 2013.

11 Lebaron P., Servais P., Troussellier M., Courties C., Vives-Rego J., Muyzer G., Bernard L., Guindulain  
12 T., Schäfer H., Stackebrandt E. : Changes in bacterial community structure in seawater mesocosm  
13 differing in their nutrient status, *Aquat. Microb. Ecol.*, 19, 255–267, 1999.

14 Lidbury, I., Johnson, V., Hall-spencer, J. M., Munn, C. B. and Cunliffe, M.: Community-level response  
15 of coastal microbial biofilms to ocean acidification in a natural carbon dioxide vent ecosystem, *Mar.*  
16 *Pollut. Bull.*, 64(5), 1063–1066, doi:10.1016/j.marpolbul.2012.02.011, 2012.

17 Lima-Mendez, G., Faust, K., Henry, N., Decelle, J., Colin, S., Carcillo, F., Chaffron, S.,  
18 Ignacio-Espinosa, J. C., Roux, S., Vincent, F., Bittner, L., Darzi, Y., Wang, J., Audic, S., Berline, L.,  
19 Bontempi, G., Cabello, A. M., Coppola, L., Cornejo-Castillo, F. M., D’Ovidio, F., De Meester, L.,  
20 Ferrera, I., Garet-Delmas, M.-J., Guidi, L., Lara, E., Pesant, S., Royo-Llonch, M., Salazar, G., Sanchez,  
21 P., Sebastian, M., Souffreau, C., Dimier, C., Picheral, M., Searson, S., Kandels-Lewis, S., Gorsky, G.,  
22 Not, F., Ogata, H., Speich, S., Stemmann, L., Weissenbach, J., Wincker, P., Acinas, S. G., Sunagawa,

1 S., Bork, P., Sullivan, M. B., Karsenti, E., Bowler, C., de Vargas, C. and Raes, J.: Determinants of  
2 community structure in the global plankton interactome, *Science* (80-. ), 348(6237), 1262073–1262073,  
3 doi:10.1126/science.1262073, 2015.

4 Liu, J., Weinbauer, M., Maier, C., Dai, M. and Gattuso, J.: Effect of ocean acidification on microbial  
5 diversity and on microbe-driven biogeochemistry and ecosystem functioning, *Aquat. Microb. Ecol.*,  
6 61(3), 291–305, doi:10.3354/ame01446, 2010.

7 Liu, N., Tong, S., Yi, X., Li, Y., Li, Z., Miao, H., Wang, T., Li, F., Yan, D., Huang, R., Wu, Y.,  
8 Hutchins, D. A., Beardall, J., Dai, M. and Gao, K.: Carbon assimilation and losses during an ocean  
9 acidification mesocosm experiment, with special reference to algal blooms, *Mar. Environ. Res.*, 129,  
10 229–235, doi:10.1016/j.marenvres.2017.05.003, 2017.

11 McDonald, D., Price, M. N., Goodrich, J., Nawrocki, E. P., DeSantis, T. Z., Probst, A., Andersen, G. L.,  
12 Knight, R. and Hugenholtz, P.: An improved Greengenes taxonomy with explicit ranks for ecological  
13 and evolutionary analyses of bacteria and archaea, *ISME J.*, 6(3), 610–618,  
14 doi:10.1038/ismej.2011.139, 2012.

15 Meron, D., Atias, E., Iasur Kruh, L., Elifantz, H., Minz, D., Fine, M. and Banin, E.: The impact of  
16 reduced pH on the microbial community of the coral *Acropora eurystoma*, *ISME J.*, 5(1), 51–60,  
17 doi:10.1038/ismej.2010.102, 2011.

18 Mielke, P. W., Berry, K. J., Brockwell, P. J. & Williams, J. S.: A class of nonparametric tests based on  
19 multiresponse permutation procedures, *Biometrika*, 68(3), 720–724, 1981. Ramaiah, N., Sarma, V. V. S.  
20 S., Gauns, M., Dileep Kumar, M. and Madhupratap, M.: Abundance and relationship of bacteria with  
21 transparent exopolymer particles during the 1996 summer monsoon in the Arabian Sea, *Proc. Indian  
22 Acad. Sci. Earth Planet. Sci.*, 109(4), 443–451, doi:10.1007/bf02708332, 2000.

1 Ray, J. L., Töpper, B., An, S., Silyakova, A., Spindelböck, J., Thyrraug, R., Dubow, M. S., Thingstad,  
2 T. F. and Sandaa, R. A.: Effect of increased pCO<sub>2</sub> on bacterial assemblage shifts in response to glucose  
3 addition in Fram Strait seawater mesocosms, *FEMS Microbiol. Ecol.*, 82(3), 713–723,  
4 doi:10.1111/j.1574-6941.2012.01443.x, 2012.

5 Roy, A.-S., Gibbons, S. M., Schunck, H., Owens, S., Caporaso, J. G., Sperling, M., Nissimov, J. I.,  
6 Romac, S., Bittner, L., Mühling, M., Riebesell, U., LaRoche, J. and Gilbert, J. a.: Ocean acidification  
7 shows negligible impacts on high-latitude bacterial community structure in coastal pelagic mesocosms,  
8 *Biogeosciences*, 10(1), 555–566, doi:10.5194/bg-10-555-2013, 2013.

9 Smith, D. C., Steward, G. F., Long, R. A. and Azam, F.: Bacterial mediation of carbon fluxes during a  
10 diatom bloom in a mesocosm, *Deep. Res. Part II*, 42(1), 75–97, doi:10.1016/0967-0645(95)00005-B,  
11 1995.

12 Sugimoto, K., Fukuda, H., Baki, M. A. and Koike, I.: Bacterial contributions to formation of  
13 transparent exopolymer particles (TEP) and seasonal trends in coastal waters of Sagami Bay, Japan,  
14 *Aquat. Microb. Ecol.*, 46(1), 31–41, doi:10.3354/ame046031, 2007.

15 Tanaka, T., Thingstad, T. F., Løvdal, T., Grossart, H.-P., Larsen, A., Schulz, K. G. and Riebesell, U.:  
16 Availability of phosphate for phytoplankton and bacteria and of labile organic carbon for bacteria at  
17 different pCO<sub>2</sub> levels in a mesocosm study, *Biogeosciences*, (5), 669–678,  
18 doi:10.5194/bgd-4-3937-2007, 2007.

19 Teeling, H., Fuchs, B. M., Becher, D., Klockow, C., Gardebrecht, A., Bennke, C. M., Kassabgy, M.,  
20 Huang, S., Mann, A. J., Waldmann, J., Weber, M., Klindworth, A., Otto, A., Lange, J., Bernhardt, J.,  
21 Reinsch, C., Hecker, M., Peplies, J., Bockelmann, F. D., Callies, U., Gerds, G., Wichels, A., Wiltshire,  
22 K. H., Glockner, F. O., Schweder, T. and Amann, R.: Substrate-Controlled Succession of Marine



1 Bacterioplankton Populations Induced by a Phytoplankton Bloom, *Science* (80-. ), 336(6081), 608–  
2 611, doi:10.1126/science.1218344, 2012.

3 Teira, E., Fernández, A., Álvarez-Salgado, X. A., García-Martín, E. E., Serret, P. and Sobrino, C.:  
4 Response of two marine bacterial isolates to high CO<sub>2</sub> concentration, *Mar. Ecol. Prog. Ser.*, 453, 27–  
5 36, doi:10.3354/meps09644, 2012.

6 Tu, Q., Yuan, M., He, Z., Deng, Y., Xue, K., Wu, L., Hobbie, S. E., Reich, P. B. and Zhou, J.: Fungal  
7 Communities Respond to Long-Term CO<sub>2</sub> Elevation by Community Reassembly, *Appl. Environ.*  
8 *Microbiol.*, 81(7), 2445–2454, doi:10.1128/AEM.04040-14, 2015.

9 Wang, Y., Zhang, R., Zheng, Q., Deng, Y., Van Nostrand, J. D., Zhou, J. and Jiao, N.:  
10 Bacterioplankton community resilience to ocean acidification: evidence from microbial network  
11 analysis, *ICES J. Mar. Sci.*, 73(3), 865–875, doi:10.1093/icesjms/fst176, 2016.

12 White P.A., Kalf J., Rasmussen J. B. and Gasol J. M.: The Effect of Temperature and Algal Biomass  
13 on Bacterial Production and Specific Growth Rate in Freshwater and Marine, *Microb. Ecol.*, 21(2), 99–  
14 118, 1991.

15 Witt, V., Wild, C., Anthony, K. R. N., Diaz-Pulido, G. and Uthicke, S.: Effects of ocean acidification  
16 on microbial community composition of, and oxygen fluxes through, biofilms from the Great Barrier  
17 Reef, *Environ. Microbiol.*, 13(11), 2976–2989, doi:10.1111/j.1462-2920.2011.02571.x, 2011.

18 Worden, A. Z., Follows, M. J., Giovannoni, S. J., Wilken, S., Zimmerman, A. E. and Keeling, P. J.:  
19 Rethinking the marine carbon cycle: Factoring in the multifarious lifestyles of microbes, *Science*  
20 (80-. ), 347(6223), 1257594–1257594, doi:10.1126/science.1257594, 2015.

21 Zhang, J., Kobert, K., Flouri, T. and Stamatakis, A.: PEAR: a fast and accurate Illumina Paired-End  
22 reAd mergeR, *Bioinformatics*, 30(5), 614–620, doi:10.1093/bioinformatics/btt593, 2014.

1 Zhang, R., Xia, X., Lau, S. C. K., Motegi, C., Weinbauer, M. G. and Jiao, N.: Response of  
2 bacterioplankton community structure to an artificial gradient of pCO<sub>2</sub> in the Arctic Ocean,  
3 Biogeosciences, 10(6), 3679–3689, doi:10.5194/bg-10-3679-2013, 2013.

4 Zhou, J., Deng, Y., Luo, F., He, Z., Tu, Q. and Zhi, X.: Functional molecular ecological networks,  
5 MBio, 1(4), e00169-10, doi:10.1128/mBio.00169-10.Editor, 2010.

6  
7  
8  
9  
10  
11  
12  
13  
14  
15  
16  
17  
18  
19  
20  
21  
22

1

2

3

## 4 **Figure legends**

5 **Figure 1** Temporal variations of  $p\text{CO}_2$  (a),  $\text{pH}_{\text{NBS}}$  (b) and Chla (c) during the whole experiment. The

6  $p\text{CO}_2$  was calculated from DIC and pH using the CO2SYS program. Data are the means  $\pm$  SD,  $n=3$ .

7

8 **Figure 2** Bacterioplankton community structure overview at different taxonomic levels during days 4, 6,

9 8, 10, 13, 19 and 29 (#1, #6, #8) under LC and HC (#2, #4, #7). X-axis represents sample name (for

10 example, D4.1 refers to bacterioplankton in mesocosm bag 1 collected at day 4) and the Y-axis

11 represents relative abundance of different groups of bacterioplankton.

12

13 **Figure 3** The relative abundance over time of primary taxa of the bacterioplankton community; HC in

14 red and LC in black. Proteobacteria (a) and Bacteroidetes (b) are phylum level; Flavobacteria (c) and

15 Alphabacteria (d) are class level; Flavobacteriales (e) and Rhodobacteriales (f) are order level;

16 Flavobacteriaceae (g) and Rhodobacteraceae (h) are family level. Data are the means  $\pm$  SD ( $n=3$ ), and the

17 asterisk represents a difference at  $p < 0.05$ .

18

19 **Figure 4** Bacterioplankton network interactions under LC (a) and HC (b) conditions. Each node

20 represents an OTU. Node colors demonstrate different taxon. Each line connects two OTUs. A blue line

21 indicates a negative interaction between nodes, suggesting predation or competition, while a red line

22 indicates a positive interaction suggesting mutualism or cooperation. OTUs with importance are marked

1 with OTU identification numbers.

2

3 **Figure 5** Sub-modules in ecological network analysis under LC (a) and HC (b) conditions. Each dot  
4 represents an OTU. The  $Z$ - $P$  plot shows OTU distribution based on their module-based topological role  
5 according to within-module ( $Z$ ) and among-module ( $P$ ) connectivity. The nodes were defined as module  
6 hubs with  $Z_i > 2.5$  and  $P_i < 0.625$ , which were more closely connected within the module, while the  
7 connectors were nodes with  $Z_i < 2.5$  and  $P_i > 0.625$  were more closely connected to nodes in other  
8 modules. Network hubs are super-generalist with a  $Z_i > 2.5$  and  $P_i > 0.625$ . The other nodes were  
9 considered peripheral.

10

11

12

13

14

15

16

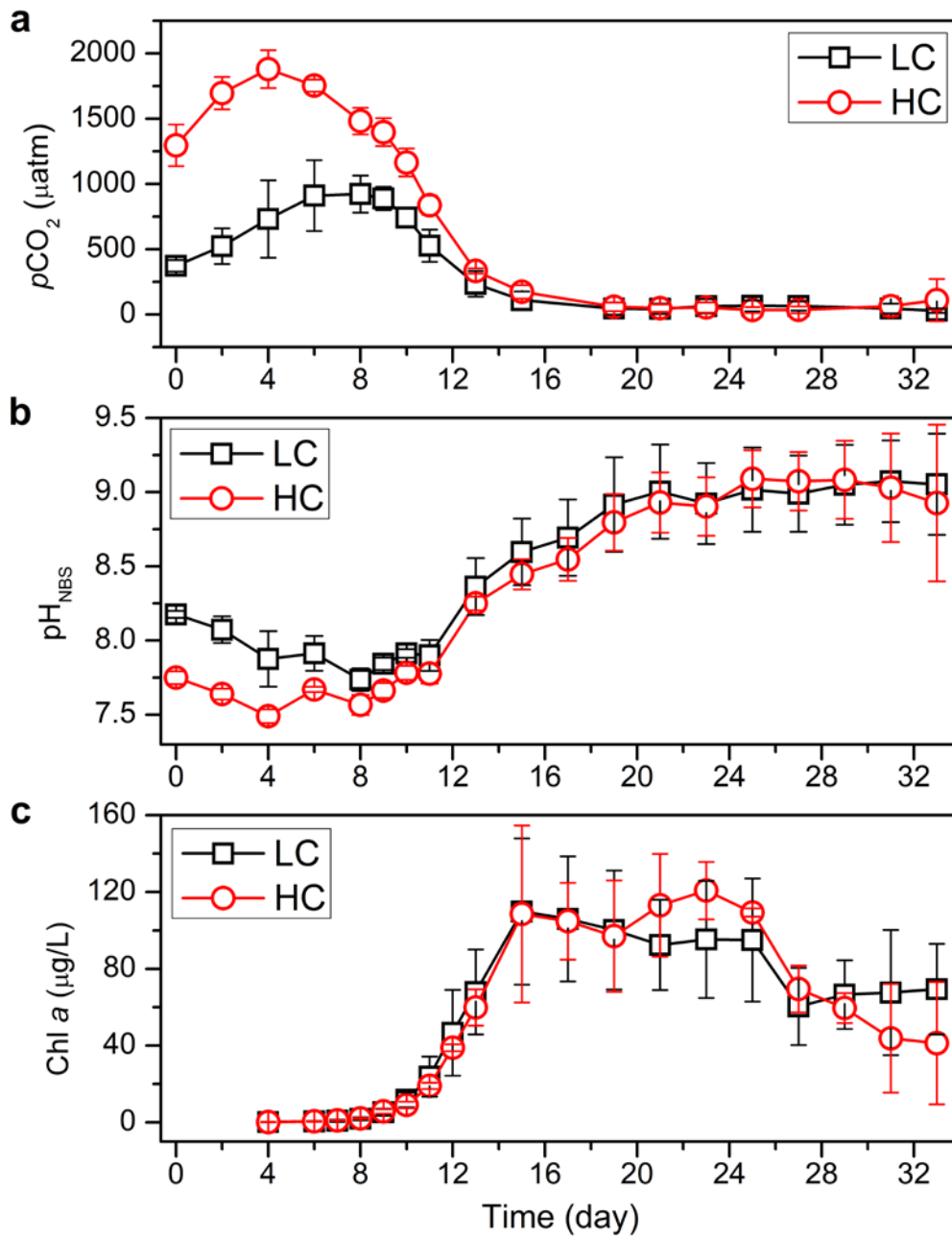
17

18

19

20

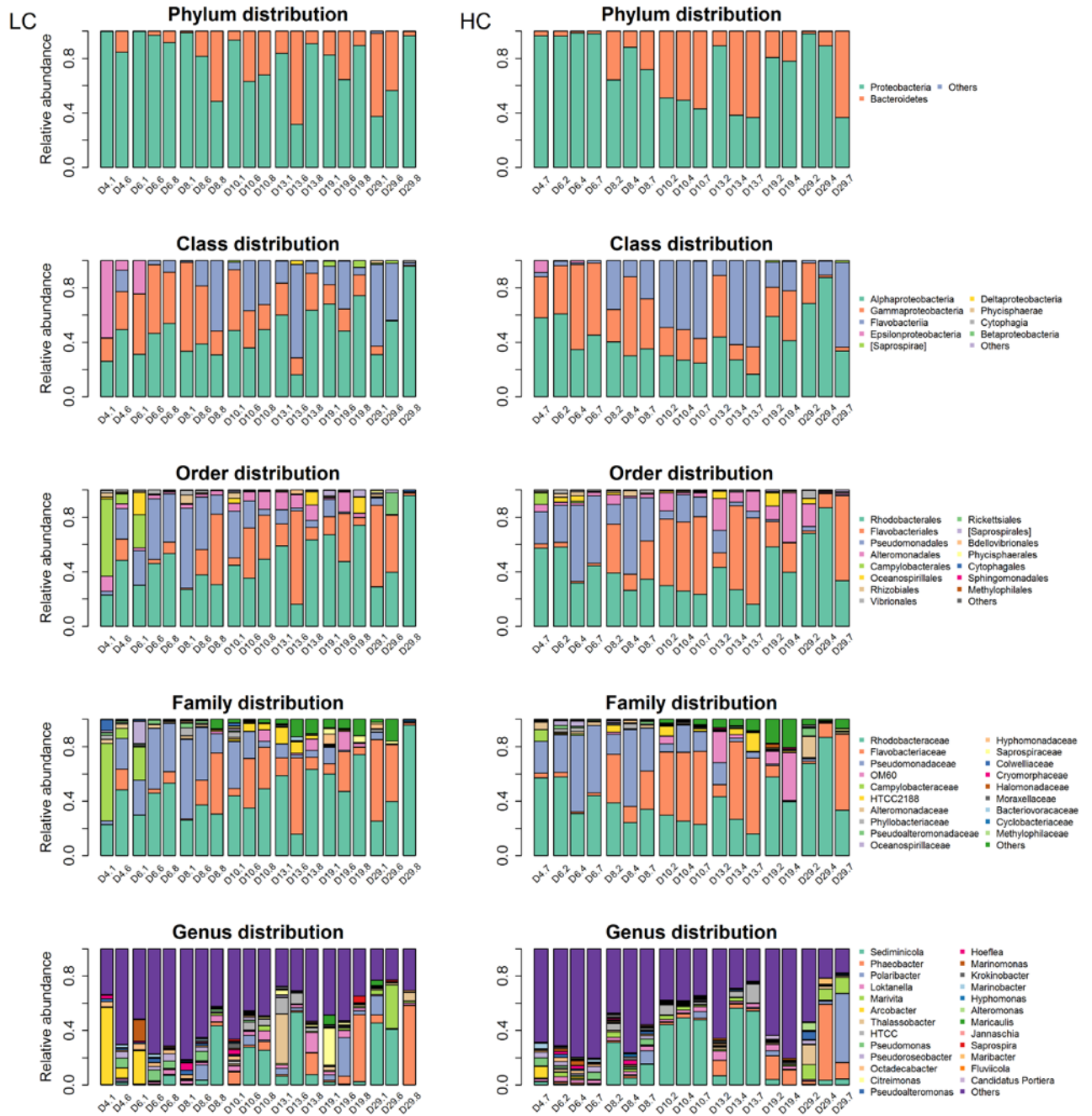
21



1

2

Figure 1



1

2

Figure 2

**Figure 3**

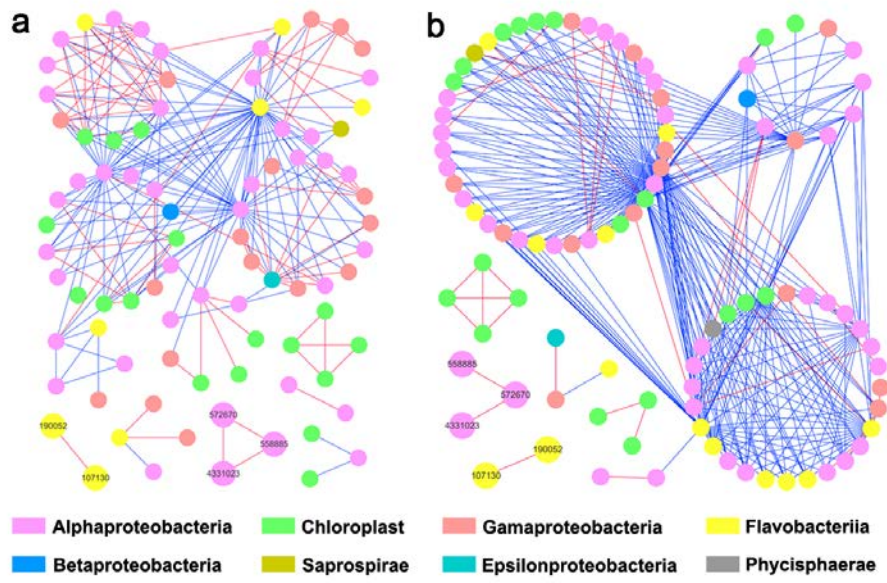


Figure 4



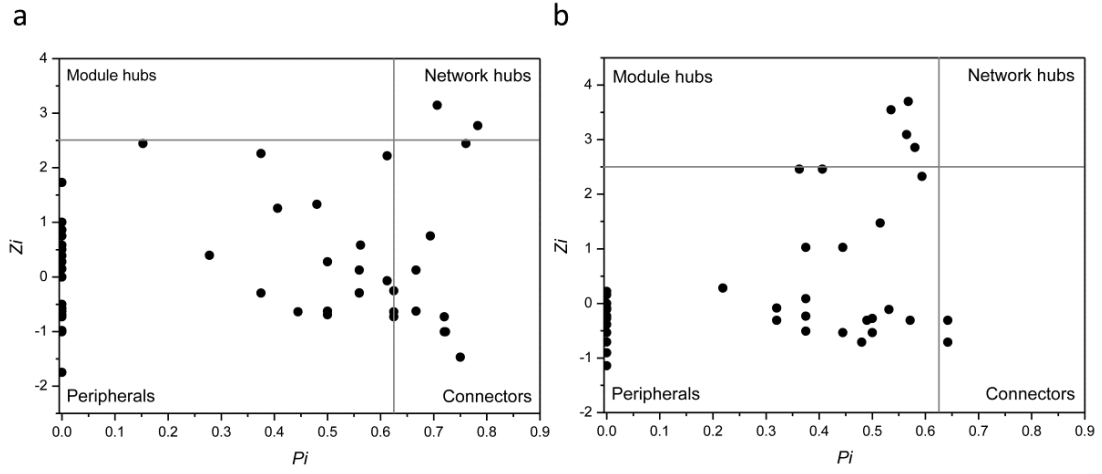


Figure 5

**Table 1** Topological properties of the bacterioplankton communities as represented by molecular networks under HC and LC treatments; also their rewired random networks.

	Experimental network						Random network			
	Total nodes	Total links	R2 of power-law	Average clustering coefficient (avgCC)	Average connectivity	Harmonic geodesic distance (HD)	Modularity	Average clustering coefficient (avgCC)	Harmonic geodesic distance (HD)	Modularity
<b>LC</b>	85	209	0.817	0.402	0.625	3.397	0.414	0.424 +/- 0.023	2.187 +/- 0.049	0.249 +/- 0.010
<b>HC</b>	96	310	0.817	0.448	0.714	2.956	0.303	0.292 +/- 0.023	2.306 +/- 0.059	0.323 +/- 0.008

**Table 2** Dissimilarity tests of bacterial communities in the HC and LC treatments at various time points.

	Anosim		MRPP		Adonis	
Time	R	P-value	$\delta$	P-value	R <sup>2</sup>	P
<b>day6</b>	-0.111	0.602	0.3952	1	0.15447	1
<b>day8</b>	0.111	0.284	0.438	0.6	0.2	0.5
<b>day10</b>	0.037	0.613	0.4929	0.7	0.17829	0.7
<b>day13</b>	0.111	0.309	0.412	0.5	0.19714	0.5
<b>day19</b>	0	0.693	0.4336	0.3	0.28263	0.3
<b>day29</b>	-0.259	1	0.4513	0.9	0.15517	0.9